A WARM-LIQUID CALORIMETER FOR COSMIC-RAY HADRONS

J. MILKE, J. ENGLER, F. FESSLER, J.R. HÖRANDEL, T. HOLST, H. KEIM, H.J. MATHES, H.H. MIELKE[a], U. RAIDT[b], J. WOCHELE

Forschungszentrum und Universität Karlsruhe, Institut für Kernphysik, P.O. Box 3640, D-76021 Karlsruhe, Germany

An iron sampling calorimeter for cosmic-ray hadrons used in the centre of the air shower experiment KASCADE is presented. The iron absorber is interspersed with eight layers of ionisation chambers filled with the room temperature liquids tetramethylsilane (TMS) and tetramethylpentane (TMP). 10 000 individual chambers filled with 17 000 litres of liquid are operating since three years. Experiences gained with the calorimeter, its performance and long-term stability are presented. For energies in the range of 0.5 TeV to 10 TeV shower profiles and transition curves have been measured and are compared with Monte Carlo calculations employing the FLUKA code.

1 Introduction

Within the extensive air shower experiment KASCADE [1], the central core of hadrons is investigated using a totally absorbing sampling calorimeter. The aim of the experiment is to determine the mass composition of primary cosmic rays in the energy domain of 10^{14} to 10^{17} eV and to measure reliably the cosmic-ray energy spectrum. The hadron content of an air shower at sea level decisively depends on the mass of the primary particle. A hadron calorimeter, therefore, is well suited to distinguish air showers initiated by different primaries.

Such a calorimeter should be able to detect hadrons of 10 TeV and more. For a good energy reconstruction it should be deeper than 10 nuclear interaction lengths λ_I. In order to distinguish individual hadrons within the core and to determine their energy seperately, a relatively fine lateral segmentation is desirable. Because of the small particle flux a calorimeter surface of 300 m^2 is needed to accumulate 100 particles per annum at 10 PeV. This is the size of the KASCADE calorimeter.

The active elements of the calorimeter consist of liquid ionisation chambers containing the liquids tetramethylsilane (TMS) and tetramethylpentane (TMP) as dielectric. The calorimeter is the first large scale device being operated using this technique. It is the intention of this article to report on the performance of the calorimeter which is taking data for three years by now, especially on the warm-liquid ionisation chambers. It is also of interest to find

[a] Now at Hewlett-Packard GmbH, Herrenbergerstrasse 135, D-71004 Böblingen, Germany
[b] Now at Alcatel SEL AG, Lorentzstrasse 10, D-70435 Stuttgart, Germany

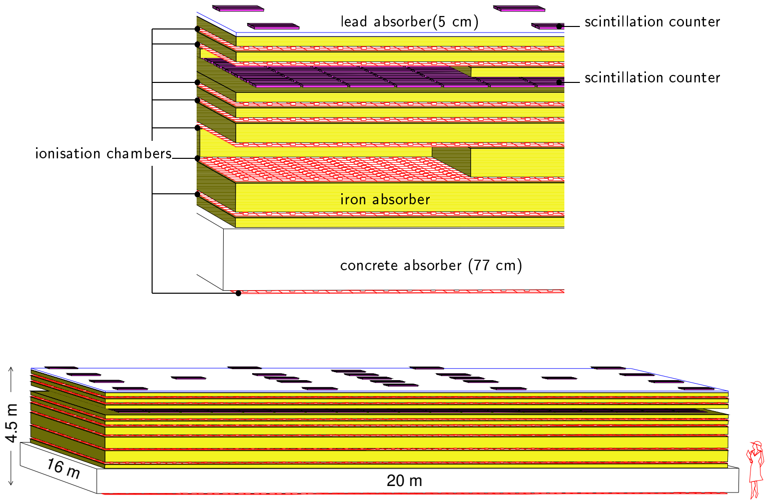

Figure 1: Schematic View of the KASCADE central calorimeter

out how well existing shower simulation codes as FLUKA [2] describe hadronic cascades in the TeV region. We cannot test the absolute amount of energy deposition due to the lack of calibration possibilities at accelerators, but we can determine the longitudinal and lateral profiles of energy deposition, thereby examining the reliability of the Monte Carlo codes.

2 Calorimeter Set-up

A sketch of the central KASCADE calorimeter is shown in Fig. 1. It is constructed from casted Fe slabs, 12 cm thick, leaving eight slots free to introduce active elements. Seven slots are filled with liquid ionisation chambers. Into the space behind the third iron layer—where hadron showers of 100 GeV reach their maximum of energy deposition—scintillation counters for fast-trigger purposes are inserted [3]. The last layer of ionisation chambers is situated below the concrete ceiling, which acts as a tail catcher of $2.5\,\lambda_I$ in thickness. The total depth of the calorimeter amounts to 11.4 interaction lengths. At an energy of 25 TeV on average 97.5 % of the energy are deposited in the calorimeter.

As can be seen from Fig. 1, sampling is constant at the top and becomes coarser, namely 24 and 36 cm, in deeper layers where the mean transition curve drops exponentially. For cosmic-ray hadrons a very good energy resolution is not mandatory at the highest energies. We therefore deliberately renounce

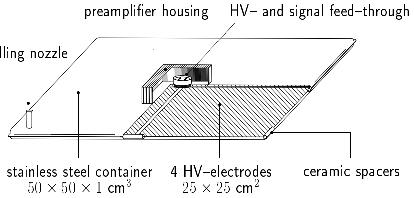

Figure 2: Sketch of a liquid ionisation chamber

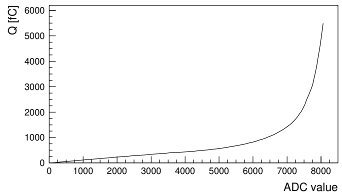

Figure 3: Signal characteristic of an amplifier chain

on the $1/\sqrt{E}$ improvement with rising energy in case of a calorimeter with constant sampling steps. Yet, when dealing with a steeply falling energy spectrum, due to the finite resolution the energy is systematically reconstructed too high. To keep the correction for this shift small, a reasonably good resolution is desirable. According to MC calculations, the calorimeter resolutions varies slowly from $\sigma(E)/E = 20\,\%$ at $100\,\mathrm{GeV}$ to $10\,\%$ at $10\,\mathrm{TeV}$.

3 Liquid Ionisation Chambers

The structure of an ionisation chamber is sketched in Fig. 2. It consists of a $50 \times 50 \times 1\,\mathrm{cm}^3$ stainless steel box containing four electrodes ($25 \times 25\,\mathrm{cm}$) positioned in the mid-plane of the box by ceramic spacers. A ceramic feed-through allows to apply high voltage to the electrodes and to read out their signals independently, ensuring the fine spatial segmentation of the calorimeter.

Several high-mobility liquids exist, which are suitable for particle detection in calorimeters [4]. For our purpose, a high signal yield and low costs were the decisive criteria, whereas a fast signal generation was of minor importance. TMS has been chosen due to its relatively favourable price. One third of the calorimeter is equipped with TMP which has been taken over from the UA1 upgrade calorimeter at CERN.

An important quantity which determines the operational capability of an ionisation chamber is the lifetime τ of free electrons in the liquid. It should be much greater than the electrons' drift time in order to collect the total charge produced. The lifetime is limited by the presence of electron-attaching impurities. Therefore, all parts of the chamber and the liquid itself have to be cleaned carefully [5].

Due to the absence of internal charge amplification, liquid ionisation detectors exhibit a linear and stable signal behaviour. A dynamic range of 1:50 000 is realised by a non-linear amplification characteristic for high pulses (Fig. 3). This insures that the signal of one passing muon up to $10\,\mathrm{GeV}$ of deposited

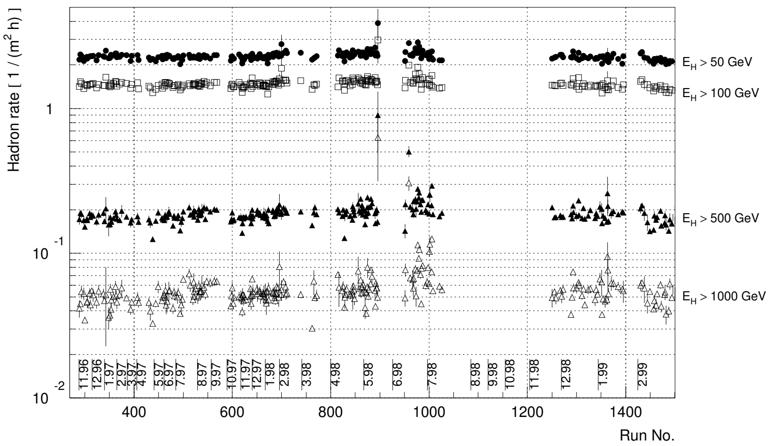

Figure 4: Average hadron rate in the calorimeter per weekly time interval. The different symbols represent the indicated threshold energies.

energy are read out without saturation.

4 Signal Stability

One of the principal motivations to use liquid ionisation chambers is their long-term stability. The electronic feed-back amplifier chain fulfills this requirement. A stability within 2 % for the first two years of running has been found. For the actual chamber signal this remains to be proven. Individual chambers, therefore, have been tested repeatedly in a triton beam at the Karlsruhe cyclotron [6]. No signal decrease has been observed.

The behaviour under constant electric field strength has been studied with the calorimeter itself. Fig. 4 shows the average rate for hadrons above the indicated energy threshold. As the flux of the cosmic-ray hadrons and the energy spectrum are known to be stable with time, the constant rate immediately reflects the signal stability of the chambers. A stable and reliable performance of the calorimeter for many years can be anticipated.

5 Longitudinal and Lateral Shower Development

Due to the lack of calibration possibilities at accelerators the energy calibration is done with a detector simulation based on the GEANT package [7] using the FLUKA code. In order to gain confidence in the simulation code we compare

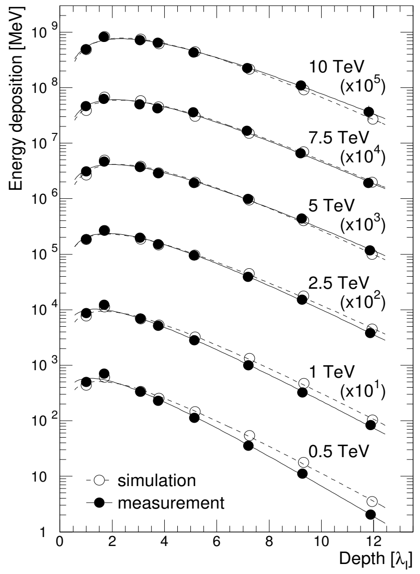

Figure 5: Measured transistion curves (full circles) compared to simulated transistion curves (open circles) using the FLUKA code. The energy depositions are multiplied by the indicated factors for a clear presentation.

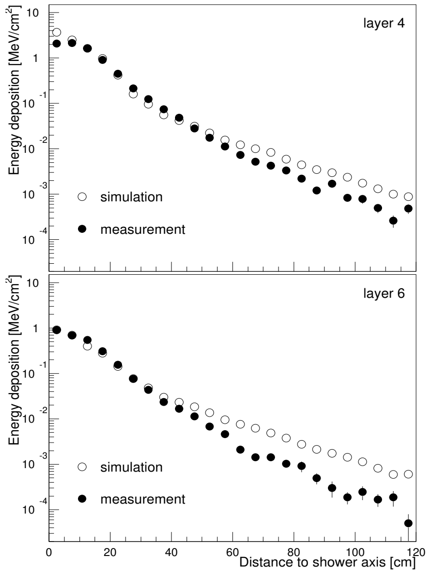

Figure 6: Energy deposition with respect to the lateral displacement from the shower axis. Mean values for 5 TeV showers in the layers 4 and 6. Measurements (full circles) compared to FLUKA simulations (open circles).

the longitudinal and lateral distributions of energy deposition of measured and simulated showers with the same reconstructed energy.

The longitudinal shower development is shown in Fig. 5. Plotted are measurements and simulations for infalling hadrons of 0.5 TeV to 10 TeV. The curves represent fits of $c \cdot t^a \cdot \mathrm{e}^{bt}$ to the data points, t being the material in nuclear interaction lengths in front of each point. This ansatz has been derived for electromagnetic cascades but can be used—as we infer from the simulations—for hadronic showers in the same way.

At the higher energies, the simulations reproduce the experimental data quite well. At lower energies the cascades seem to enter deeper into the absorber. However, this is probably an artifact caused by instrumental effects. At these energies the energy deposition in a chamber is low and still in the MeV region where the amplifier noise cannot be neglected. In the simulation it is taken into account as a mean value with a Gaussian distribution. This may not be realistic enough to simulate the data correctly. Consequently, the slight differences should not be taken as major discrepancies.

A comparison of lateral energy distributions as obtained by measurements and simulations is shown in Fig. 6. Presented is the decrease of energy deposition of layers 4 and 6, which are situated deep enough not to be influenced by accompanying electromagnetic radiation created somewhere in the air above the detector. The experimental findings are well reproduced by the simulations in the cascade core up to a distance of about 35 cm. This is the radius of a cylinder around the shower axis where 90 % of the hadron energy is found, and approximately corresponds to the effective absorption length of the calorimeter structure, calculated to be $\lambda_{eff} = 29$ cm. The flattening in the very centre within 10 cm is an instrumental effect due to the finite pad size of 25 cm.

At larger distances the measured showers indicate smaller amounts of deposited energy than the simulation. It is a small effect that does not influence the central energy determination. However, it is observed in all layers and at all energies. As a result, hadron cascades overlap less strongly and individual hadrons in dense jets of particles or in cosmic-ray shower cores can be seperated more easily.

Acknowledgments

The authors would like to thank all members of the KASCADE collaboration for making the data used available. Special thanks go to many colleagues who helped to make the large calorimeter work successfully, in particular Daniela Boos, Heike Deris, Wolfgang Paulus, Michael Riegel, Doris Wochele, Peter Ziegler, and many others. Without their engagement and enthusiasm the enormous task of constructing the calorimeter would not have been accomplished.

References

1. H.O. Klages et al., *Nucl. Phys.* B (Proc. Suppl.) **52 B** (1997) 92
2. P.A. Aarmio et al., FLUKA user's guide. Technical Report, **TIS-RP-190**, CERN (1987,1990)
3. M. Brendle and U. Raidt, *Nucl. Instrum. Methods* A **412** (1998) 420
4. J. Engler, Fast Liquid Ionisation Chambers at Room Temperatures, *J. Phys.* G.: Nucl. Part. Phys. **22** (1996) 1-23
5. J. Engler et al., A warm-liquid calorimeter for cosmic-ray hadrons, *Nucl. Instrum. Methods* A **427** (1999) 528
6. J. Engler et al., *Nucl. Instrum. Methods* A **311** (1992) 479 and *Nucl. Instrum. Methods* A **327** (1993) 128
7. GEANT 3.15, Detector Description and Simulation Tool, CERN Program Library Long Writeup W5013, CERN (1993)